Photocatalysis of the Reaction between Ammonia and Nitric Oxide on TiO$_2$ Surfaces

NOEL W. CANT[1] AND JOHN R. COLE

School of Chemistry, Macquarie University, New South Wales 2109, Australia

The photocatalytic reaction between ammonia and nitric oxide on TiO$_2$ wafers under near ultraviolet illumination has been investigated. The reaction produces nitrogen and nitrous oxide with a ratio slightly above two. When $^{15}NH_3$ and ^{14}NO are used, $^{14}N^{15}N$ and $^{14}N^{14}NO$ are formed almost exclusively. Comparative measurements have been made for the related photocatalytic reaction between ammonia and oxygen, and for nitric oxide photodecomposition. The rate of the latter is approximately one-sixth that of the ammonia plus nitric oxide reaction. It yields nitrogen and nitrous oxide with a ratio less than 0.5 and is accompanied by some deposition of nitrates on the TiO$_2$ wafer. The ammonia plus oxygen reaction is of intermediate rate and is also accompanied by nitrate formation. The nitrogen/nitrous oxide ratio is approximately four when using 10 Torr of each reactant. Both reactions involving ammonia exhibit a small deuterium kinetic isotope effect, the rate ratio for NH$_3$ versus ND$_3$ being about 1.3. Nitrous oxide production is zero order in ammonia and shows a Langmuir-like dependence on oxidant pressure. Both oxidation reactions exhibit similarly curved Arrhenius plots with low apparent activation energies. The dependencies on light intensity are nonlinear, with an apparent order of approximately 0.6 in both cases. A model which can explain the overall characteristics of the three reactions is presented. © 1992 Academic Press, Inc.

INTRODUCTION

Titanium dioxide, particularly its anatase modification, is the best known heterogeneous photocatalyst (i.e., a substance which acts as a catalyst only when its surface is illuminated). It is particularly effective for the oxidation of organic molecules and simple inorganic gases. This activity is undesirable in the context of paint films containing TiO$_2$ pigments (*1*) but is potentially useful as a means for monitoring and destruction of refractory organics in water (*2–4*). Details of the mechanism of such photocatalytic reactions on surfaces remain unclear. Recently Turchi and Ollis (*5*) have argued persuasively that the active oxidant in aqueous systems is a surface formed hydroxyl radical. For gas–solid systems there is good evidence from ESR measurements for the formation of O$_2^-$ under illumination (*6*).

However, it is more usually assumed that O$^-$ is the active agent for the oxidation of simple hydrocarbons (*7*) and carbon monoxide (*8*). It may also be involved in oxygen isotope exchange, although direct involvement of lattice oxygen is also implicated (*8*).

The method of attack on the substrate, and the subsequent reaction pathways, is even less certain. In part this is because the best studied systems are rather too simple (e.g., carbon monoxide oxidation or isotope exchange) to offer paths for tracing or else so complex (total oxidation of large organics) that tracing is impractical. Here we report an investigation of the photocatalyzed reaction between ammonia and nitric oxide over TiO$_2$ in which it has been possible to infer with some confidence how the products are derived. Apart from a brief report in the older literature (*9*) we can find no previous studies of photocatalysis of this reaction. However, the thermally catalyzed counterpart is of great importance for the

---

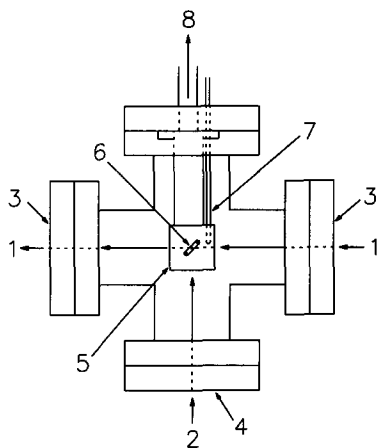[1] To whom correspondence should be sent.

FIG. 1. Details of combination photoreactor and infrared cell: (1) beam of infrared spectrometer, (2) ultraviolet beam, (3) CaF_2 windows, (4) type 7056 glass window, (5) sample holder, (6) TiO_2 wafer, (7) thermocouple well, (8) to vacuum system.

removal of nitrogen oxides from the stack gases of power stations by the $DeNO_x$ process (10). A wealth of mechanistic information concerning it is available for a wide variety of catalysts including V_2O_5/TiO_2 (11, 12), Cr_2O_3 (13), Fe_2O_3 (14), CuO (15), and Pt (16). In addition, there have been previous studies of the TiO_2 photocatalyzed oxidation of ammonia (9, 17) and of the photocatalyzed decomposition of nitric oxide (18, 19). The photocatalytic oxidation of amines in semiconductor suspensions has also been investigated (20, 21), as has the reduction of dinitrogen to ammonia in irradiated heterogeneous systems (22–24). This work includes remeasurement of some of the characteristics of ammonia oxidation and nitric oxide decomposition under different conditions and an overall evaluation of the connection between the three photocatalytic systems.

EXPERIMENTAL

The photocatalytic experiments were carried out in a reaction chamber based on a standard 70-mm UHV cross (Fig. 1). Two opposite ports were fitted with flanged calcium fluoride windows of 3-mm thickness (Harshaw, Inc.), which transmitted above 1000 cm^{-1} in the infrared. A flanged-type 7056 glass window (Perkin–Elmer ULTEK) transmitting down to 260 nm in the ultraviolet was fitted to a third port. The fourth comprised a metal flange with a vacuum connection on one side and an aluminium block sample holder screwed to a stainless steel support on the other. A hole drilled in the holder enabled placement of a thermocouple close to the sample. The entire chamber was mounted on a ceramic post such that the sample beam of a Perkin–Elmer Model 580 spectrometer traversed the two calcium fluoride windows and a channel cut through the sample holder. The glass window faced a 100-W mercury lamp filtered by a heat absorbent glass filter (Schott KG1) and a black glass filter (Schott UG1). The combination isolated the 300–400 nm region (in effect the 365 nm Hg line), which was focused by a quartz lens onto the entrance to a second channel cut into the aluminium block at right angles to that for the spectrometer beam. Test experiments with a thermistor-type radiometer (Yellow Springs Inst., Model 65A with 6551 probe) showed that the near ultraviolet beam intensity was ≈ 40 mW cm^{-2} where the channels crossed. In some experiments the beam intensity was reduced by a set of calibrated fine wire grids placed away from the focus. Checks showed that sample illumination remained uniform. The reaction chamber was heated by four 120-W collar heaters which provided temperatures to 300°C when covered by an insulated box.

The samples consisted of pressed wafers of TiO_2 (Cab-o-Ti, Cabot Corp., 85% anatase, 15% rutile, surface area 50 m^2/g). They were cut to a size of 20 mm × 10 mm, giving a weight of 50 ± 5 mg. The samples were fitted into a vertical slot cut into the sample holder at 45° to each of the channels at the position where they crossed. In this way it was possible to record the infrared spectrum of the wafer while it underwent ultraviolet illumination. Prior to installation in the holder, each wafer was heated in air over-

night at 400°C to burn off residual hydrocarbons and rehydrated in water vapor for a minimum of 20 h. It was further treated in the reaction chamber by evacuation for 2h at $\approx$ 25°C. It was then equilibrated with a small excess of ammonia and the excess ammonia was pumped. A known pressure of ammonia followed by a known pressure of oxidant was admitted, and the system was allowed to stand (usually overnight) to allow complete mixing. Blank experiments showed that no reaction occurred during this period. The wafer was then illuminated by the mercury lamp for a fixed period (from ½ to 24 h). After illumination the gaseous contents of the chamber were allowed to expand into a series of U-tube traps. By cooling the traps to different temperatures, and careful manipulation, two fractions, one comprising N$_2$ plus O$_2$ and the other N$_2$O alone, were separated out. The pressure of each fraction in a known volume was measured with a precision capacitance manometer (MKS Instruments Type 77). The identity of each fraction was confirmed by mass spectrometry using an AEI MS12 instrument. In this way the number of moles of the nitrogen-containing products could be determined. It was also possible to follow N$_2$O product formation continuously by measurement of the growth of its gaseous infrared band in the region from 2050 to 2300 cm^{-1}. While this was convenient as a means of following reaction, the conversion from absorbance to pressure in the chamber was complex, since calibration showed that the Beer–Lambert plot exhibited a curvature which was dependent on the composition of the chamber contents.

The oxygen, ammonia, nitrous oxide, and nitric oxide used were standard CP grade from cylinders. The oxygen was purified by passage through a silica gel trap held at −80°C, while the others were purified by repeated trap to trap transfer. The only measurable impurity was a small amount of residual nitrous oxide in the nitric oxide, for which a correction was made when calculating that produced by reaction. The ND$_3$

(>99%D) and ^{15}NH$_3$ ($\approx$93% ^{15}N) were obtained from Merck, Sharp, and Dohme (Montreal). The distribution of ^{15}N in the nitrogen-containing products for reactions involving ^{15}NH$_3$ was determined by mass spectrometry, with the mass spectrometer operated with sufficient resolution to separate compounds with the same unit mass (e.g., ^{12}C^{16}O and ^{14}N^{14}N at 28, ^{15}N^{15}N and ^{14}N^{16}O at 30, etc.).

RESULTS

In blank experiments on the three reactions studied, no products were observed during illumination of gaseous reactant mixtures in the absence of a TiO$_2$ sample, and with TiO$_2$ present, reaction took place only under illumination with band gap radiation (300–400 nm). Visible light was not effective. In addition, no oxidation occurred when TiO$_2$ was illuminated with only ammonia, or ammonia plus nitrous oxide, present. Similarly, nitrous oxide alone did not decompose significantly in the presence of illuminated TiO$_2$.

Characteristics of NH$_3$/NO Reaction

Figure 2 shows the time dependence of N$_2$O and N$_2$ production when TiO$_2$ wafers were illuminated in the presence of mixtures comprising 10 Torr of NH$_3$ and 10 Torr of NO. The closed squares show N$_2$O production for four separate experiments with one wafer using different illumination times. They correspond closely to the open squares obtained from sequential infrared measurements of the gaseous N$_2$O band at 2235 cm^{-1} made during the longest of the four runs. The open and closed circles show N$_2$O and N$_2$ production, each measured by separation, for a second set of four experiments with a different wafer. The ratio of N$_2$ to N$_2$O is slightly over two for each experiment and thus independent of illumination time.

All four curves in Fig. 2 show a similar fall off in rate with time. Two factors contribute to this, reactant depletion (28% of the NO consumed after 4 h) and product
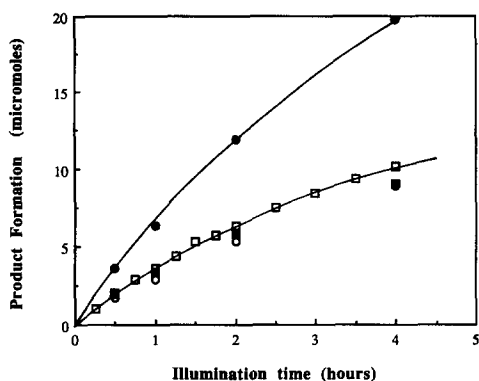
FIG. 2. Nitrous oxide and nitrogen production as a function of time during photocatalysis of the ammonia plus nitric oxide reaction on an illuminated TiO_2 wafer at $\approx 30°C$ with initial pressures of 10 Torr of NH_3 and 10 Torr of NO: ■, N_2O production measured by collection in four separate experiments with different illumination times; □, N_2O production measured by infrared spectroscopy; ○, and ●, N_2O and N_2 production measured by collection in a separate set of four experiments with a different wafer.

inhibition. Calculations using the pressure-dependence data presented later indicated that the latter was more important. Separate experiments with N_2O and N_2 added to the starting mixture showed that they did not inhibit. On the other hand, water did inhibit, probably by competition with ammonia for surface sites. This inhibition was not permanent, since repeat experiments with intervening evacuation for 1 h at $\approx 25°C$ gave identical results to those of Fig. 2. Dibble and Raupp (25) have similarly reported water inhibition of a gas–solid photocatalyzed reaction in their study of trichloroethylene oxidation.

A further series of experiments using a variety of conditions were carried out to establish if the N_2/N_2O ratio was constant. Results are shown in Table 1. With the exception of the final experiment in which only adsorbed ammonia was present, the N_2/N_2O ratio is independent of illumination time and the pressure of either reactant within experimental error. The average value is 2.18 ($\sigma = 0.08$). Four runs with ND_3 gave a small kinetic isotope effect ($k_H/k_D \approx 1.3$) com-

pared to that expected for a process in which the slow step is breaking a N–H(D) bond ($k_H/k_D \approx 9$ at 30°C (26)). Thus the rate-determining step is not bond cleavage in ammonia.

Figure 3 shows the pressure dependence of N_2O production. (These results correspond to a further set of experiments with another wafer, in which the initial pressure of each reactant was in turn held constant and the pressure of the other varied). The reaction is zero order in NH_3 and exhibits the Langmuir shape for NO with the order decreasing with pressure (a log–log plot gave an apparent order of 0.23). Overall the kinetics conform to the dual site model proposed by Mozzanega et al. (17) for the photocatalytic reaction of ammonia and oxygen over TiO_2, i.e.,

rate (to N_2O) =

$$k \cdot \frac{K_{NO}P_{NO}}{1 + K_{NO}P_{NO}} \cdot \frac{K_{NH_3}P_{NH_3}}{1 + K_{NH_3}P_{NH_3}},$$

where k is the rate constant and the K's are adsorption coefficients. If $K_{NH_3}P_{NH_3} \gg 1$ this reduces to

$$\text{rate} = k_p \cdot \frac{K_{NO}P_{NO}}{1 + K_{NO}P_{NO}},$$

$$\text{with } k_p = k \cdot \frac{K_{NH_3}P_{NH_3}}{1 + K_{NH_3}P_{NH_3}},$$

which produces the observed behavior. One expects P_{NO}/rate versus P_{NO} to be linear, and that was true (correlation coefficient = 1.00), and the value of K_{NO} derived from the slope of the plot was 0.23 $Torr^{-1}$. The possibility of an Eley–Rideal reaction between an adsorbed species and gaseous ammonia can be ruled out due to the independence of N_2O production from NH_3 pressure.

Four experiments were carried out with $^{15}NH_3/^{14}NO$ mixtures to determine the origin of the nitrogen atoms in the nitrogen-containing products. Illumination was continued for longer than in the experiments

TABLE 1

Nitrogen and Nitrous Oxide Production under Various Conditions during Photocatalysis of Mixtures of Ammonia and Nitric Oxide on Illuminated TiO₂ at ≈30°C

Illumination time (hour)	Initial pressures		N_2 produced (μmol)	N_2O produced (μmol)	N_2 produced/ N_2O produced
	NH_3 (Torr)	NO (Torr)			
2	5.1	5.0	9.1	3.93	2.32
2	5.1	9.8	10.7	4.94	2.16
2	10.2	9.8	11.9	5.35	2.23
2	10.0	5.0	9.0	4.07	2.22
2	20.0	9.9	12.2	5.45	2.24
2	10.1	19.7	13.4	6.09	2.19
1	10.2	9.9	6.3	2.87	2.18
0.5	10.1	9.9	3.6	1.71	2.09
2	9.7	2.1	5.9	2.73	2.16
4	10.1	9.9	19.8	8.87	2.23
2	10.0	2.0	5.0	2.46	2.01
2	10.0	1.0	3.5	1.64	2.16
2	10.1	9.9	11.8	5.43	2.17
2	a	10.0	5.7	3.41	1.68

a No gas phase ammonia present. The TiO₂ wafer was equilibrated with 10 Torr of NH₃ and evacuated for 2 h at ≈25°C prior to admission of NO.

described previously in order to maximize the accuracy of the isotope determinations. Results are shown in Table 2. In each case the nitrous oxide contains no ¹⁵N and is therefore derived entirely from nitric oxide (the 1% ¹⁴N¹⁵NO can be attributed to naturally occurring ¹⁵N in the nitric oxide—0.37% per nitrogen atom). By contrast the nitrogen is predominantly ¹⁴N¹⁵N. No ¹⁵N¹⁵N or ¹⁵N¹⁶O was observed. If the raw analytical data shown are corrected for the 7% ¹⁴NH₃ present in the starting ammonia, then for the first three experiments (in which ammonia gas was present) 97 ± 2% of the

TABLE 2

Distribution of ¹⁵N in the Nitrogen-Containing Products from Photocatalysis of Mixtures of ¹⁵N Labeled Ammonia (93% ¹⁵NH₃) and ¹⁴NO on Illuminated TiO₂ at ≈30°C

Illumination time (hour)	Initial pressures		Product distribution (%)			
	¹⁵NH₃ (Torr)	¹⁴NO (Torr)	Nitrogen		Nitrous Oxide	
			¹⁴N¹⁴N	¹⁴N¹⁵N	¹⁴N¹⁴NO	¹⁵N¹⁴NO
11	10.3	20.5	12	88	99	1
17	10.2	20.4	8	92	99	1
17	10.2	10.3	10	90	99	1
24	a	20.0	22	78	99	1

a No gas phase ammonia present. The TiO₂ wafer was equilibrated with 10 Torr of ¹⁵NH₃ and evacuated for 2 h prior to admission of ¹⁴NO.
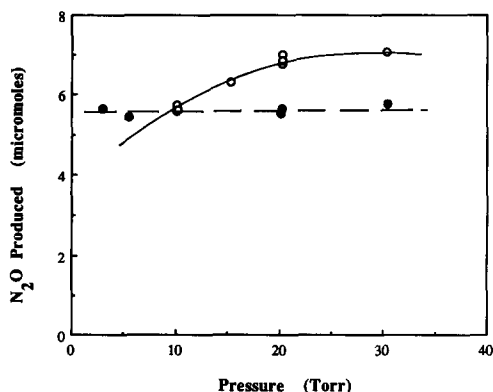
FIG. 3. Nitrous oxide production over a 2-h period as a function of reactant pressures during photocatalysis of mixtures of ammonia and nitric oxide on illuminated TiO_2 at $\approx 30°C$: ●, dependence on NH_3 pressure with NO pressure of 10.2 Torr; ○, dependence on NO pressure with NH_3 pressure of 10.2 Torr.

nitrogen derives one atom from ^{14}NO and one from $^{15}NH_3$. The remaining 3% derives both atoms from the nitric oxide. These results are very like those for the corresponding thermally catalyzed reaction over Fe_2O_3 (14) and some types of Cr_2O_3 (13), but distinctly different to those for V_2O_5 (12), CuO (15), and Pt (16), over which substantial amounts of $^{14}N^{14}N$ and $^{15}N^{14}NO$ are formed.

The final experiment in Table 2 used adsorbed ammonia alone (i.e., the wafer was equilibrated with $^{15}NH_3$ and pumped for a short while before admitting ^{14}NO) and the results are somewhat different. After correction for the presence of $^{14}NH_3$, 85% of the nitrogen derives one nitrogen atom from each source, and 15% derives both atoms from nitric oxide.

Photocatalytic Decomposition of NO

Table 3 gives results for successive experiments in which a TiO_2 wafer was illuminated for 2 h in the presence of 10 Torr of NO alone. The rate of N_2O formation declined for the first three experiments but was then constant. The accuracy of the N_2 determinations is insufficient to show the same trend. The N_2/N_2O ratio is 0.38 ± 0.15, much lower than the value of 2.2 found for

photocatalysis of the NH_3 plus NO reaction. Decomposition of NO to N_2O and N_2 would be expected to produce oxygen as well, but none was detected. It is likely that oxygen reacts with NO in the gas phase to produce NO_2 which then readsorbs on the wafer and elsewhere in the system. Infrared spectra of the TiO_2 wafer during the course of the experiments showed steady growth in bands attributable to nitrate species.

Lines six to nine of Table 3 give results for four successive NH_3 plus NO experiments made after the NO photodecomposition ones. The rate of N_2O formation in the first one is a bit lower than ones listed for similar conditions in Table 1. However, the succeeding ones have comparable rates. It is likely that deposition of NO_2 during the NO decomposition consumes some hydroxyl groups which are restored by the water produced during the first NH_3 plus NO experiment. The final column of Table 3 shows the rate at which NO is photoreacted in the two types of experiment, based on the N_2O and N_2 produced, and assuming that the NH_3 plus NO reaction produces nitrogen and nitrous oxide in the ratio of two with all the nitrogen atoms in the nitrous oxide, and half of those in the nitrogen, derived from NO. The NH_3 plus NO reaction is approximately six times as fast as NO decomposition on this basis.

The final row of Table 1 shows the result of a single NH_3 plus NO experiment in which NH_3 was present on the TiO_2 surface alone. The N_2/N_2O ratio is below that found with gaseous NH_3 present, as one might expect if the reaction involves a combination of the NH_3 plus NO reaction and NO photodecomposition.

Characteristics of NH_3/O_2 Reaction

This reaction was more difficult to study for two reasons. Firstly, unlike the NH_3 plus NO one, it gave rise to solid as well as gaseous products. The solids were observed as trace deposits on the interior walls of the system and by infrared spectroscopy of the TiO_2 wafer, which showed a continuous

TABLE 3

Comparison of Photocatalytic Decomposition of Nitric Oxide and Photocatalysis of
Mixtures of Ammonia and Nitric Oxide on TiO$_2$ at ≈30°C[a]

Initial pressures		N$_2$ produced (μmol)	N$_2$O produced (μmol)	N$_2$ produced/ N$_2$O produced	rate (μmol(NO)/hr)
NH$_3$ (Torr)	NO (Torr)				
—	10.4	0.4	1.9	0.2	2.3
—	10.3	0.8	1.6	0.5	2.4
—	10.3	0.5	1.2	0.4	1.7
—	10.3	0.4	1.2	0.3	1.6
—	10.4	0.6	1.2	0.5	1.8
10.1	10.3	[b]	4.5	[b]	9.0
10.2	10.2	[b]	5.3	[b]	10.6
10.1	10.1	[b]	5.4	[b]	10.8
10.3	10.2	[b]	5.2	[b]	10.4

[a] The experiments were run successively in the order given with intervening evacuations for
1 h at ≈25°C. The illumination time was 2 h in each case.
[b] Not determined.

growth in nitrate bands as reaction proceeded. It seems likely that the NH$_3$ plus O$_2$ reaction produces some NO which reacts with O$_2$ in the gas phase to produce NO$_2$ which is deposited throughout the system. The amount of solid matter formed was not quantifiable. A further problem arose in the procedure used to separate the gaseous products formed during each run. The noncondensable fraction comprised both product N$_2$ and unreacted O$_2$. The amount of N$_2$ could be determined only by mass spectrometry, and that technique was not available during many runs. Attention was therefore concentrated on N$_2$O formation, as compared to that formed during the NH$_3$ plus NO reaction, and the existing results of Mozzanega et al. (17) for the NH$_3$ plus O$_2$ reaction under quite different conditions (continuous flow reactor versus batch reactor here).

Table 4 shows results for some experiments with both reactions of ammonia in which N$_2$ formation was measured as well as N$_2$O formation. For the NH$_3$/O$_2$ reaction the N$_2$/N$_2$O ratio was 4.2 ± 0.4. Mozzanega et al. (17) reported values that increased with NH$_3$ pressure from 2 to 7 over the range

30 to 250 Torr. Changes in O$_2$ pressure had no effect on the N$_2$/N$_2$O ratio under their conditions, and experiments with varying NH$_3$ and O$_2$ pressures in our system gave the same result. The data of Table 4 also show two other effects. First the N$_2$/N$_2$O ratio (3.0 ± 0.2) for the NH$_3$/NO reactions is greater than for those shown in Table 1 (2.2 ± 0.2). It is likely that some photoadsorbed oxygen is retained by the TiO$_2$ during the mild evacuation following each NH$_3$ plus O$_2$ reaction and that this contributes to product formation during the subsequent NH$_3$ plus NO reactions. Second, the carrying out of an NH$_3$ plus NO reaction seems to reduce the rate of N$_2$O formation in the following NH$_3$ plus O$_2$ experiment. It is possible that some photoadsorbed NO is carried over from the NH$_3$/NO run and that this reacts with gaseous oxygen under illumination to form NO$_2$ bound to a reaction site with consequent inhibition of reaction. The NH$_3$ plus O$_2$ reaction did not inhibit subsequent NH$_3$ plus NO reactions in the same way, even though the former deposits nitrate as noted previously. However, in that case the nitrate is deposited generally throughout the system, indicating that the NO$_2$ responsible

TABLE 4

Comparison of Photocatalytic Reactions of Ammonia plus Oxygen and Ammonia plus Nitric Oxide Mixtures on Illuminated TiO_2 at $\approx 30°C$[a]

Initial pressures			N_2 produced (μmol)	N_2O produced (μmol)	N_2 produced/ N_2O produced
NH_3 (Torr)	O_2 (Torr)	NO (Torr)			
10.3	9.8	—	16	4.2	3.8
10.3	9.7	—	21	4.6	4.5
10.2	—	9.8	33	10.3	3.2
10.2	—	9.8	31	10.3	3.0
10.2	9.8	—	16	3.6	4.4
10.3	9.8	—	15	3.6	4.2
10.2	—	9.8	29	10.1	2.9

[a] The experiments were run sequentially in the order shown with intervening evacuations for 1 h at $\approx 25°C$. The illumination time was 4 h in each case.

for it is formed homogeneously and not specifically on the photocatalytic reaction site. A much more extensive set of alternating reactions in which N_2O formation alone was followed also showed inhibition of NH_3 plus O_2 reactions by prior NH_3 plus NO reactions but not vice versa.

Figure 4 shows the effect of variations in O_2 and NH_3 pressure on the rate of N_2O formation over TiO_2. As for the NH_3 plus
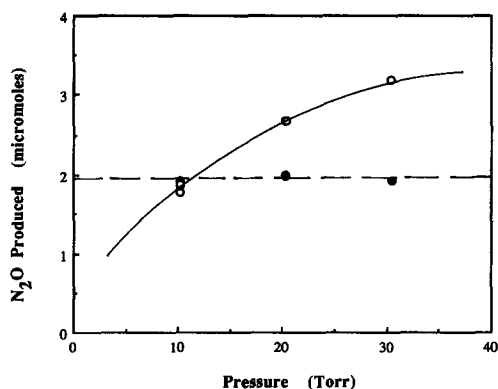
FIG. 4. Nitrous oxide production over a 2-h period as a function of reactant pressures during photocatalysis of mixtures of ammonia and oxygen on illuminated TiO_2 at $\approx 30°C$: ●, dependence on NH_3 pressure with O_2 pressure of 10.3 Torr; ○, dependence on O_2 pressure with NH_3 pressure of 10.3 Torr.

NO reaction, the dependence is zero order in NH_3 and exhibits a Langmuir-type shape for oxygen. These dependencies also fit the dual site model shown earlier. Table 5 compares kinetic parameters derived for the two reactions together with the information reported by Mozzanega et al. (17). The similarity between the two reactions in respect of N_2O formation is clear. The slightly higher apparent kinetic order for the NH_3 plus O_2 reaction can be attributed to a lower value for the adsorption coefficient of the oxidant ($K_{O_2} \approx 0.05$ Torr^{-1} compared to $K_{NO} \approx 0.23$ Torr^{-1}). This indicates that NO is adsorbed slightly more strongly than is O_2. The two reactions seem to differ in respect to N_2 formation. Our measurements for the NH_3 plus NO reaction show that N_2 and N_2O formation depends on oxidant pressure alone. The results of Mozzanega et al. (17), which we have no reason to doubt, indicate that N_2 formation from NH_3 plus O_2 mixtures depends on the pressure of ammonia as well.

Temperature Dependence

Figure 5 shows Arrhenius plots for the temperature dependence of N_2O formation during the two photocatalytic oxidations. They exhibit similar curvature and the ap-

TABLE 5

Apparent Reaction Orders and Kinetic Parameters for the Photocatalyzed Reactions between Ammonia and Nitric Oxide and between Ammonia and Oxygen

System	Dependence on	Apparent reaction order		Adsorption coefficient (Torr^{-1})[c]
		to N$_2$	to N$_2$O	
NH$_3$ + NO	NH$_3$	zero	zero	≥4
(this work)	NO	0.2	0.2	0.23
NH$_3$ + O$_2$	NH$_3$	[a]	zero	≥4
(this work)	O$_2$	[a]	0.5	0.05
NH$_3$ + O$_2$	NH$_3$	0.5	zero	[a]
Ref. (17)	O$_2$	0.3	0.4	0.02

[a] Not determined.
[b] Estimated from data in Ref. (17) for the pressure range 30 to 250 Torr.
[c] For N$_2$O production.

parent activation energies ($\approx$20 kJ/mol at 30°C and <10 kJ/mol at 100°C) are very low, as is common for photocatalytic reactions. The curvature probably reflects a reduction in coverage of sites by oxidant as the temperature is raised, since adsorption coefficients are expected to decrease with increase in temperature.

Effect of Illumination Intensity

Experiments were carried out in which the light intensity falling on the TiO$_2$ wafer

from the mercury lamp was reduced by a set of calibrated fine wire grids. Figure 6 shows plots of the variation in N$_2$O production with illumination intensity for the two reactions of ammonia. There is a similar curvature for the two reactions, indicating that the photocatalytic rates are not directly proportional to the light intensity. Log–log plots were linear. The value of n (the slope of the line) in the equation
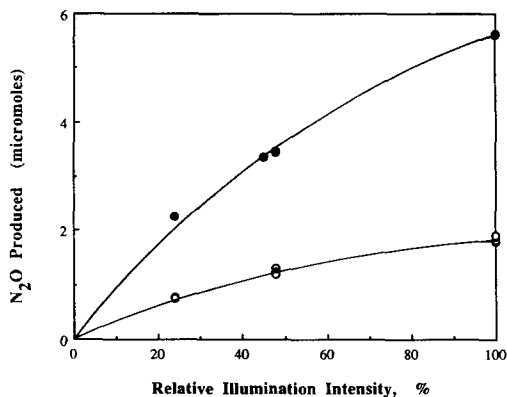

FIG. 5. Arrhenius plots for the photocatalytic production of nitrous oxide on illuminated TiO$_2$: ●, ammonia plus nitric oxide reaction; ○, ammonia plus oxygen reaction.

FIG. 6. Dependence of photocatalytic production of N$_2$O over a 2-h period on relative light intensity over illuminated TiO$_2$ at $\approx$30°C: ●, ammonia plus nitric oxide reaction; ○, ammonia plus oxygen reaction. The photon flux for 100% light intensity was 7 × 10^{16} photons cm^{-2}s^{-1}.

Apparent Quantum Yields for Photocatalysis of the Ammonia plus Nitric Oxide, Ammonia plus Oxygen, and Nitric Oxide Decomposition Reactions over Illuminated TiO_2 at $\approx 30°C$ with Initial Reactant Pressures of 10 Torr Each

	Apparent quantum yields		
	NH_3 + NO	NH_3 + O_2	NO decomposition
Over 0.5 hours illumination			
definition 1[a]	0.026	0.013	—
definition 2[b]	0.035	0.021	—
Over 2.0 hours illumination			
definition 1[a]	0.015	0.008	0.0018
definition 2[b]	0.020	0.013	0.0036

[a] Nitrogen-containing molecules (N_2 and N_2O) produced per incident photon.
[b] NO (or O_2) molecules consumed (calculated according to reaction stoichiometry) per incident photon.

$$\text{rate} = k\Phi^n,$$

where Φ, the light intensity, is 0.64 for the NH_3 plus NO reaction and 0.60 for the NH_3 plus O_2 one. In these experiments the total number of photons received by the sample in the different experiments varied (since the illumination time was constant), and there is some possibility for bias since reactant conversions varied. A further set of experiments was carried out in which product formation was assessed after time intervals which equalized the number of incident photons. Again for both reactions N_2O formation exhibited a dependence on light intensity which was closer to 0.5 than unity.

Relative Rates and Quantum Yields

The relative rates for the three reactions can be compared in terms of quantum yield, the number of reactant molecules consumed (or product molecules produced) as a fraction of the number of photons absorbed. In the present systems quantum yields cannot be compared unambiguously, since the reaction stoichiometries vary and some products go unmeasured as solid deposits. Table 6 gives apparent values calculated for two different definitions, one in terms of nitrogen-containing molecules produced, the other in terms of NO (or O_2) molecules con-

sumed. The absolute values are unlikely to be very accurate, principally due to uncertainties in the measurement of the number of photons incident at the sample position and the likelihood that a varying fraction are reflected rather than absorbed by the wafer. Evenso the values are lower than reported for other simple photocatalytic oxidations on TiO_2 (e.g., 0.1 for isobutane (27) and also 0.1 for propene (28)). The relative values should however be fairly accurate, and they indicate that the rate ratio for the three reactions, NH_3 plus NO : NH_3 plus O_2 : NO decomposition, is approximately $8:4:1$ according to definition 1 and $6:4:1$ for definition 2. The origin of this order is discussed later.

DISCUSSION

The principal findings concerning the two photocatalytic reactions of NO studied here are as follows.
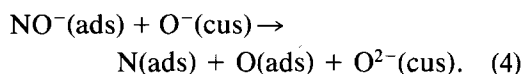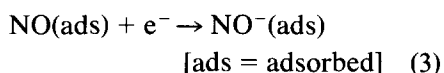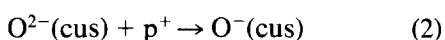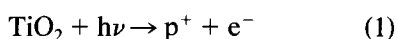
(i) Nitric oxide by itself is photodecomposed on illuminated TiO_2, but the rate is considerably slower than its reaction with ammonia under the same conditions.

(ii) The N_2/N_2O ratio produced by the NH_3 plus NO reaction has a fixed value close to two. The ratio is much lower for
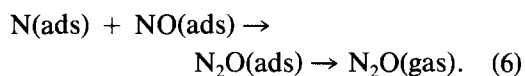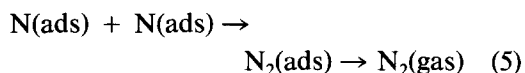
NO decomposition and varies with pressure.

(iii) The nitrous oxide produced during the NH$_3$ plus NO reaction is derived entirely from NO, but each nitrogen molecule derives one atom from NO and one from NH$_3$.

The most reasonable interpretation is that the initial step for both reactions is light induced dissociation of NO and that the presence of ammonia introduces an additional pathway to nitrogen. Courbon and Pichat (18) have proposed that NO dissociation on illuminated TiO$_2$ proceeds as follows:

$$TiO_2 + h\nu \rightarrow p^+ + e^- \quad (1)$$

$$O^{2-}(cus) + p^+ \rightarrow O^-(cus) \quad (2)$$

$$NO(ads) + e^- \rightarrow NO^-(ads)$$
$$[ads = adsorbed] \quad (3)$$

$$NO^-(ads) + O^-(cus) \rightarrow$$
$$N(ads) + O(ads) + O^{2-}(cus). \quad (4)$$

They based this scheme on the suggestion of Cunningham et al. (29) that photoinduced holes (p$^+$) were localized at coordinatively unsaturated oxide ions, O^{2-}(cus), and their own observations (19) that the adsorption of NO reduced photoconductivity. Courbon and Pichat (18) did not propose pathways by which N$_2$ and N$_2$O were formed, but the obvious ones are

$$N(ads) + N(ads) \rightarrow$$
$$N_2(ads) \rightarrow N_2(gas) \quad (5)$$

$$N(ads) + NO(ads) \rightarrow$$
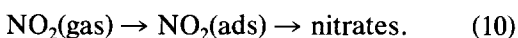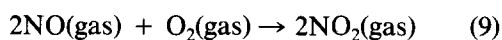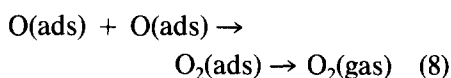$$N_2O(ads) \rightarrow N_2O(gas). \quad (6)$$

The ratio of N$_2$ to N$_2$O should decline as the pressure of NO, and hence its surface coverage, is increased as is observed.
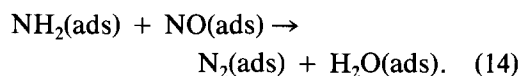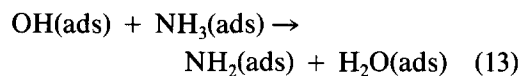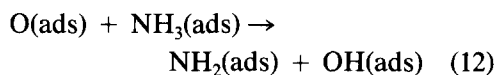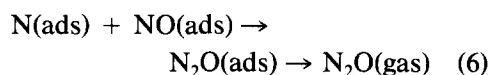
Nitrates could arise similarly via

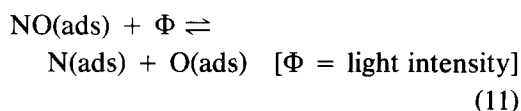$$NO(ads) + O(ads) \rightarrow$$
$$NO_2(ads) \rightarrow nitrates \quad (7)$$
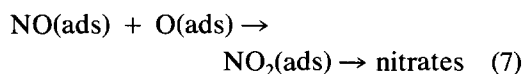
or by combination of oxygen atoms, desorption of the O$_2$ produced, oxidation of NO in the gas phase, and deposition of NO$_2$,

$$O(ads) + O(ads) \rightarrow$$
$$O_2(ads) \rightarrow O_2(gas) \quad (8)$$

$$2NO(gas) + O_2(gas) \rightarrow 2NO_2(gas) \quad (9)$$

$$NO_2(gas) \rightarrow NO_2(ads) \rightarrow nitrates. \quad (10)$$

If steps (1) to (4) above were all irreversible and surface coverages were low, then the overall photocatalytic rate would be linear with light intensity. However, if step (1) is an equilibrium then a square-root dependence is expected. Egerton and King (30) reported such a situation for the photocatalytic oxidation of neat isopropanol over TiO$_2$, as did Okamoto et al. (31) for liquid phase phenol oxidation. The same square-root dependence would apply if all four steps are at equilibrium. There is some evidence for the reversibility of step (4) in that it allows for the photocatalytic exchange reaction known to occur between ^{15}N^{18}O and Ti^{16}O$_2$ (18).

The near to 2 : 1 N$_2$/N$_2$O ratio, and the ^{15}N isotope results, for the NO + NH$_3$ reaction can be explained by the following scheme:

$$NO(ads) + \Phi \rightleftharpoons$$
$$N(ads) + O(ads) \quad [\Phi = light\ intensity]$$
$$\quad (11)$$

$$N(ads) + NO(ads) \rightarrow$$
$$N_2O(ads) \rightarrow N_2O(gas) \quad (6)$$

$$O(ads) + NH_3(ads) \rightarrow$$
$$NH_2(ads) + OH(ads) \quad (12)$$

$$OH(ads) + NH_3(ads) \rightarrow$$
$$NH_2(ads) + H_2O(ads) \quad (13)$$

$$NH_2(ads) + NO(ads) \rightarrow$$
$$N_2(ads) + H_2O(ads). \quad (14)$$

Here reaction (11) is simply a convenient summary for the NO dissociation steps outlined above. The essence of the scheme is that each N(ads) produces one N$_2$O molecule derived from nitric oxide only as required by the isotope experiments. The O(ads) are scavenged by ammonia rather than produce nitrates as occurs when am-

monia is absent. Most crucially, since the scavenging occurs in two steps with intervening formation of OH, each O(ads) gives rise to *two* NH_2 species, each of which gives one nitrogen molecule by reaction with adsorbed NO. Overall the N_2/N_2O ratio should be two, and every nitrogen molecule should contain one atom from each source, as observed. If scavenging of O(ads) is fast then no nitrates should be observed and the reaction should be faster than for decomposition of NO alone. The fact that the N_2/N_2O ratio is slightly greater than two can be attributed to a small amount of nitrogen atom pairing (reaction (5)). Reaction (14) may seem rather improbable since it involves the simultaneous breaking of three bonds, and the making of three more, but it is a well known elementary process in the gas phase (*32, 33*). Theoretical calculations show that the potential energy wells for the rearrangement are very shallow (*34, 35*). Reactions (12) and (13) are also well established gas phase elementary processes (*36*).

Rate expressions can be derived on the basis of the above model by making the steady state assumption. If the photodissociation is a rapid equilibrium (i.e., $k_{-11} \gg k_6, k_{12}$) then the expression is

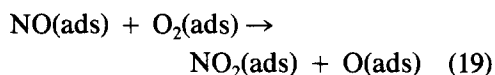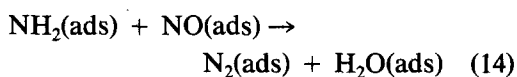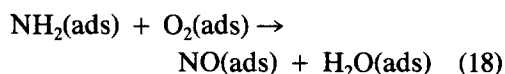$$\text{rate} = 3k_6^{1/2}k_{12}^{1/2}K^{1/2}\Phi^{1/2}\Theta_{NH_3}^{1/2}\Theta_{NO}, \quad (15)$$
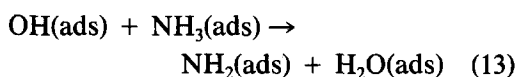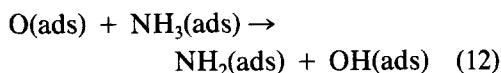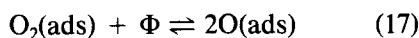
where the subscripted k's refer to the rate constants for the correspondingly numbered reactions, $K = k_{11}/k_{-11}$, and the Θ's are the coverages of the adsorption sites for NO and NH_3. The reaction should be half order in light intensity, zero order in ammonia if the adsorption sites for the adsorbate are fully occupied, and of Langmuir dependence on NO if its adsorption is of that isotherm type. The experimental findings are close to that. The corresponding rate equation if the photodissociation is nonreversible (i.e., $k_{-11} \ll k_6, k_{12}$) is
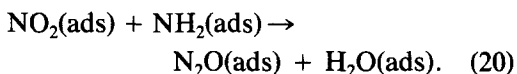
$$\text{rate} = 3k_6\Phi\Theta_{NO}. \quad (16)$$

This also predicts zero order kinetics in NH_3 and the Langmuir isotherm shape for NO,

but a linear dependence on light intensity. The observed dependence of rate on $\Phi^{0.64}$ implies either a situation midway between these extremes or that the data have been collected at a sufficiently high light intensity that electron–hole recombination is significant (*30, 31*). In the former case one would expect the small deuterium kinetic isotope effect that is observed on the grounds that k_{12} involves NH bond breaking and it occurs to the $\frac{1}{2}$ power in Eq. (15) and is absent from Eq. (16).

The close similarity between the NH_3 plus NO photocatalytic reaction and the NH_3 plus O_2 one suggests that the same type of chemistry is involved. The following scheme is proposed:

$$O_2(ads) + \Phi \rightleftharpoons 2O(ads) \quad (17)$$

$$\begin{aligned} O(ads) + NH_3(ads) &\rightarrow \\ &NH_2(ads) + OH(ads) \quad (12) \end{aligned}$$

$$\begin{aligned} OH(ads) + NH_3(ads) &\rightarrow \\ &NH_2(ads) + H_2O(ads) \quad (13) \end{aligned}$$

$$\begin{aligned} NH_2(ads) + O_2(ads) &\rightarrow \\ &NO(ads) + H_2O(ads) \quad (18) \end{aligned}$$

$$\begin{aligned} NH_2(ads) + NO(ads) &\rightarrow \\ &N_2(ads) + H_2O(ads) \quad (14) \end{aligned}$$

$$\begin{aligned} NO(ads) + O_2(ads) &\rightarrow \\ &NO_2(ads) + O(ads) \quad (19) \end{aligned}$$

[or $NO(ads) \rightarrow NO_2(ads) \rightarrow$ nitrates by reactions (7), (8), (9), and (10) as before]

$$\begin{aligned} NO_2(ads) + NH_2(ads) &\rightarrow \\ &N_2O(ads) + H_2O(ads). \quad (20) \end{aligned}$$

The oxygen dissociation step (17) could proceed similarly to that outlined earlier for NO i.e., formation of O_2^- with dissociation to 2O(ads) on coordinatively unsaturated O^{2-}. The O(ads) then reacts with adsorbed ammonia to give an NH_2 species as with the NH_3 + NO reaction. Reaction (18) is analogous to (14) and yields NO(ads). Once formed NO(ads) may react in two ways. One path leads to nitrogen by the same process occurring in the NH_3 plus NO reaction. The

other reaction is oxidation to NO_2, which can then produce nitrous oxide via reaction (20). The latter is again a well known fast reaction in the gas phase (36). Alternatively, the NO_2 can also adsorb as nitrates in the same manner as applies for the NO photodecomposition reaction.

Mozzanega et al. (17) have proposed a completely different set of pathways for the NH_3 + O_2 reaction with NH_3O, NH, and HNO as intermediates. The present scheme is believed to be more reasonable on the grounds of consistency with the NH_3 plus NO reaction and the involvement of reactions which have well established counterparts in elementary gas phase processes.

It is not possible to derive rate expressions for the above scheme for the NH_3 plus O_2 reaction without making assumptions regarding the mechanism by which some of the NO(ads) is oxidized to NO_2 and some of the latter to nitrates. However, some general comparisons between the two reactions of ammonia can be made. If the photocatalytic rate is primarily controlled by reactions (1) and (2) (i.e., the formation of holes and electrons and the capture of the hole by a coordinatively unsaturated oxide ion) then the reaction rates should be similar. Table 6 shows that this is true within a factor of two regardless of the method used to define the quantum yield. If the availability of adsorbed oxidant molecule, (NO(ads) or O_2(ads)), for electron capture according to step (3) (and its equivalent with oxygen) is also rate influencing, then the rate should be lower with oxygen, since the calculated value for its adsorption coefficient ($K_{O_2} \approx$ 0.05 $Torr^{-1}$) is less than that for nitric oxide ($K_{NO} \approx$ 0.23 $Torr^{-1}$). Two further factors may influence the rate of the NO reaction relative to the O_2 one. The probability of electron capture from an electron–hole pair could depend on the electron affinity of the oxidant. However, if this effect were present it would be expected to produce a higher rate with O_2 since, at least in the gas phase, the electron affinity of O_2 (43 kJ/mol) is much greater than that NO (2.5 kJ/mol) (37).

A more likely contribution to the rate difference is that the reaction scheme with NO results in the production of three nitrogen-containing molecules (two N_2 and one N_2O) per nitric oxide molecule dissociated. With O_2 the combined yield of N_2 and N_2O is at most two per O_2 photodissociated. Any diversion to nitrates, as is observed, will reduce that. For the photodecomposition of NO in the absence of ammonia at most one N_2O or 0.5 N_2 molecules can result per dissociation event. The presence of adsorbed NH_3 also restricts the reverse step in reaction (11) by scavenging the atomic oxygens (reaction (12)) as they are formed, thereby increasing the rate over that observed for NO photodecomposition alone. Thus the trend in quantum yields in Table 6 can be semiquantitatively accounted for in terms of the different stoichiometries by which the initially dissociated molecule is converted to gaseous nitrogen-containing product molecules.

In the present work pathways and surface species have been inferred on the basis of kinetic and isotope measurements. Infrared spectroscopic measurements made concurrently were not successful in providing direct evidence for reaction intermediates, presumably because their concentrations were below the detection limits. However, the measurements did provide information concerning stable adsorbed species, especially surface nitrates produced as a byproduct of the ammonia/oxygen reaction. These results will be reported separately, together with some data on the effect of hydroxyl group concentration.

REFERENCES

1. Völz, H. G., Kaempf, G., Fitzky, H. G., and Klaeren, A., in "Photodegradation and Photostabilization of Coatings" (S. P. Pappas and F. H. Winslow, Eds.), ACS Symposium Series, No. 151, p. 163. American Chemical Society, Washington, D.C., 1981.
2. Ollis, D. F., Pelizzetti, E., and Serpone, N., in "Photocatalysis: Fundamentals and Applications" (N. Serpone and E. Pelizzetti, Eds.), p. 603. Wiley, New York, 1989.

3. Matthews, R. W., *J. Catal.* **111**, 264 (1988).
4. Abdullah, M., Low, G. K.-C., and Matthews, R. W., *J. Phys. Chem.* **94**, 6820 (1990), and references therein.
5. Turchi, C. S., and Ollis, D. F., *J. Catal.* **122**, 178 (1990).
6. Anpo, M., Aikawa, N., Kubokawa, Y., Che, M., Louis, C., and Giamello, E., *J. Phys. Chem.* **89**, 5689 (1985).
7. Courbon, H., Formenti, M., and Pichat, P., *J. Phys. Chem.* **81**, 550 (1977).
8. Sato, S., and Kadowaki, T., *J. Catal.* **106**, 295 (1987).
9. McLean, W. R., and Ritchie, M., *J. Appl. Chem.* **15**, 452 (1965).
10. Bosch, H., and Janssen, F. J. J. G., *Catal. Today* **2**, 369 (1987).
11. Ramis, G., Busca, G., Bregani, F., and Forzatti, P., *Appl. Catal.* **64**, 259 (1990).
12. Miyamoto, A., Kobayashi, K., Inomata, M., and Murakami, Y., *J. Phys. Chem.* **86**, 2945 (1982).
13. Niiyama, H., Murata, K., and Echigoya, E., *J. Catal.* **48**, 201 (1977).
14. Niiyama, H., Ookawa, T., and Echigoya, E., *Nippon Kagaku Kaishi*, 1871 (1975).
15. Otto, K., and Shelef, M., *J. Phys. Chem.* **76**, 37 (1972).
16. Otto, K., Shelef, M., and Kummer, J. T., *J. Phys. Chem.* **74**, 2690 (1970).
17. Mozzanega, H., Herrmann, J. M., and Pichat, P., *J. Phys. Chem.* **83**, 2251 (1979).
18. Courbon, H., and Pichat, P., *J. Chem. Soc. Faraday Trans. 1* **80**, 3175 (1984).
19. Pichat, P., Courbon, H., Disdier, J., Mozzanega, M. N., and Herrmann, J. M., *in* "Proceedings, 7th International Congress on Catalysis Tokyo, 1980" (T. Seiyama and K. Tanabe, Eds.), Pt. B, p. 1498. Elsevier, Amsterdam, 1981.
20. Fox, M. A., and Younathan, J. N., *Tetrahedron* **42**, 6285 (1986).
21. Ohtani, B., Osaki, H., Nishimoto, S., and Kagiya, T., *Chem. Lett.*, 1075 (1985).
22. Schiavello, M., and Sclafani, A., *in* "Photoelectrochemistry, Photocatalysis, and Photoreactors" (M. Schiavello, Ed.), p. 503. Reidel, 1985.
23. Augugliaro, V., and Palmisano, L., *in* "Photocatalysis and Environment: Trends and Applications" (M. Schiavello, Ed.), p. 425. Kluwer, 1988.
24. Soria, J., Conesa, J. C., Augugliaro, V., Palmisano, L., Schiavello, M., and Sclafani, A., *J. Phys. Chem.* **95**, 274 (1991).
25. Dibble, L. A., and Raupp, G. B., *Catal. Lett.* **4**, 345 (1990).
26. Melander, L., "Isotope Effects on Reaction Rates." Ronald Press, New York, 1960.
27. Djeghri, N., Formenti, M., Juillet, F., and Teichner, S. J., *Faraday Discuss. Chem. Soc.* **58**, 185 (1974).
28. Pichat, P., Herrmann, J. M., Disdier, J., and Mozzanega, M. N., *J. Phys. Chem.* **83**, 3122 (1979).
29. Cunningham, J., Doyle, B., and Leahy, E. M., *J. Chem. Soc. Faraday Trans. 1* **75**, 2000 (1979).
30. Egerton, T. A., and King, C. J., *J. Oil Colour Chem. Assoc.* **62**, 386 (1979).
31. Okamoto, K.-I., Yamamoto, Y., Tanaka, H., and Itaya, A., *Bull. Chem. Soc. Jpn.* **58**, 2023 (1985).
32. Whyte, A. R., and Phillips. L. F., *Chem. Phys. Lett.* **102**, 451 (1983).
33. Silver, J. A., and Kolb, C. E., *J. Phys. Chem.* **91**, 3713 (1987).
34. Gilbert, R. G., Whyte, A. R., and Phillips, L. F., *Int. J. Chem. Kinet.* **18**, 721 (1986).
35. Harrison, J. A., MacLagan, R. G. A. R., and Whyte, A. R., *J. Phys. Chem.* **91**, 6683 (1987).
36. Lesclaux, R., *Rev. Chem. Intermed.* **5**, 347 (1984).
37. Travers, M. J., Cowles, D. C., and Ellison, G. B., *Chem. Phys. Lett.* **164**, 449 (1989).